1967

The effect of condensation on the pressure distribution around a cylinder.

Ovrom, Allan Alfred.

Massachusetts Institute of Technology

THE EFFECT OF CONDENSATION ON THE PRESSURE DISTRIBUTION AROUND A CYLINDER

ALLAN ALFRED OVROM, Jr.

Thesis Supervisor: Peter Griffith
Title: Associate Professor of Mechanical Engineering

19 May 1967

THE EFFECT OF CONDENSATION ON THE PRESSURE DISTRIBUTION AROUND A CYLINDER

by

ALLAN ALFRED OVROM, JR.

LIEUTENANT, UNITED STATES NAVY

B.S., United States Naval Academy

(1959)

Submitted in Partial Fulfillment of the

Requirements for the Degree of

Naval Engineer and the Degree of

Master of Science in Mechanical Engineering

at the

MASSACHUSETTS INSTITUTE OF TECHNOLOGY

May, 1967

THE EFFECT OF CONDENSATION ON THE PRESSURE DISTRIBUTION AROUND A CYLINDER

by

Allan Alfred Ovrom, Jr., Lieutenant, United States Navy

Submitted to the Department of Naval Architecture and Marine Engineering on 19 May, 1967, in partial fulfillment of the requirements for the degree of Master of Science in Mechanical Engineering and the professional degree, Naval Engineer.

ABSTRACT

An investigation was carried out to determine the effect of condensation on the pressure distribution around a right cylindrical cylinder in cross flow. A single cylinder in an infinite flow and a cylinder with nearby walls were analyzed for comparison with the test section data. It was found that condensation does alter the pressure distribution with larger rates of condensation.

A vertical test section orientation was used to facilitate correlation with general condensors and to aid in condensate removal.

The condensation was found to behave in a manner analogous to boundary layer suction thus causing the profile of pressure coefficient to move toward the ideal solution and the points of separation to move nearer the wake stagnation point. With this analogy to boundary layer suction, steam devices such as diffusers and condensors may be designed more efficiently.

Thesis Supervisor: Peter Griffith
Title: Associate Professor of Mechanical Engineering

ACKNOWLEDGMENTS

The author wishes to express his sincere appreciation to Professor Peter Griffith, his thesis advisor, for his guidance and encouragement throughout this investigation.

The helpful advice and service of technician Fred Johnson on the experimental apparatus are also gratefully acknowledged.

TABLE OF CONTENTS

LIST OF FIGURES AND TABLES

FIGURES

TABLES

NOMENCLATURE

A - area in ft^2.

D - diameter in in.

g - local acceleration of gravity in ft./sec.

g_o - gravitational constant 32.17 $\frac{lbm\text{-}ft.}{lbf\text{-}sec.^2}$

h - manometer levels.

I - principal meter constant.(6)

$\dot{m}$ - mass rate of flow in lbm./sec.

N_R - Reynold's Number based on diameter.

P - pressure in lbf./$in.^2$.

Q - flow rate in $ft.^3$/sec.

R - radius in in.

S.G. - specific gravity of fluid.

T - temperature in ^oC.

v - specific volume in $ft.^3$/lbm.

V - velocity in ft./sec.

Greek Letters

β - diameter ratio

ρ - density lbm./$ft.^3$

μ - viscosity (lbm./hr.-ft.)

ψ - stream function

θ - angle (^{o})

γ - specific weight lbf./$ft.^3$.

CHAPTER I

INTRODUCTION

The purpose of this investigation was to determine whether or not any condensation of a steam boundary layer would cause the pressure distribution through the layer to change. If the large volumetric change occurring with the condensation of steam could be used to reduce the boundary layer thickness, perhaps the phenomenon could be used to produce more favorable pressure gradients in steam devices, less drag on objects in steam flow, or reduction in the size of steam condensing devices.

For example, a common steam device, the steam diffuser, might be designed more efficiently. In the case of expanding section area devices, the diffuser can have separation occurring along its walls because of the adverse pressure gradients. Manual extraction of mass along the walls will reduce the adverse pressure gradient and retard separation.

One possible geometry for a diffuser is a vertical axis of flow and porous condensing walls. Any condensation would be removed with the assistance of gravity and the pressure gradient created across the diffuser wall. A porous wall could be constructed with a tightly spiralled expanding cone of small diameter copper tubing.

As a vehicle for the demonstration of this phenomenon the right cylindrical cylinder was chosen. The literature abounds with theoretical and experimental studies of the flow patterns, pressure distributions, drag coefficients, etc. of a cylinder in a uniform streaming flow.

Mathematical solutions for the velocity distribution around a cylinder in a streaming flow with and without circulation or solutions to the Navier-Stokes equations for small Reynold's Number flows are found in texts by Lamb[1], Milne-Thompson[2], and Schlichting[3].

The exact solution to the steady state boundary layer equations for the flow past a cylinder as solved by Blasius is contained in Schlichting. Drag and viscous data from various experiments are found in Schlichting, Rohsenow and Choi[4] and Robertson[5]. Some of the experimental pressure coefficient data as presented in Robertson is found in Figure I. A more detailed analysis of the use of images to produce walls in a streaming flow around a cylinder is outlined in Robertson.

The simple solution for the velocity distribution around a cylinder in a streaming flow and a similar solution using two images are outlined in Chapter II.

The pressure distribution around a cylinder in a streaming flow is best characterized by a pressure coefficient which is defined as:

$$C_p = \frac{P}{1/2\ \rho\ V_o^2}$$

FIGURE I

PRESSURE COEFFICIENT DISTRIBUTIONS (5)

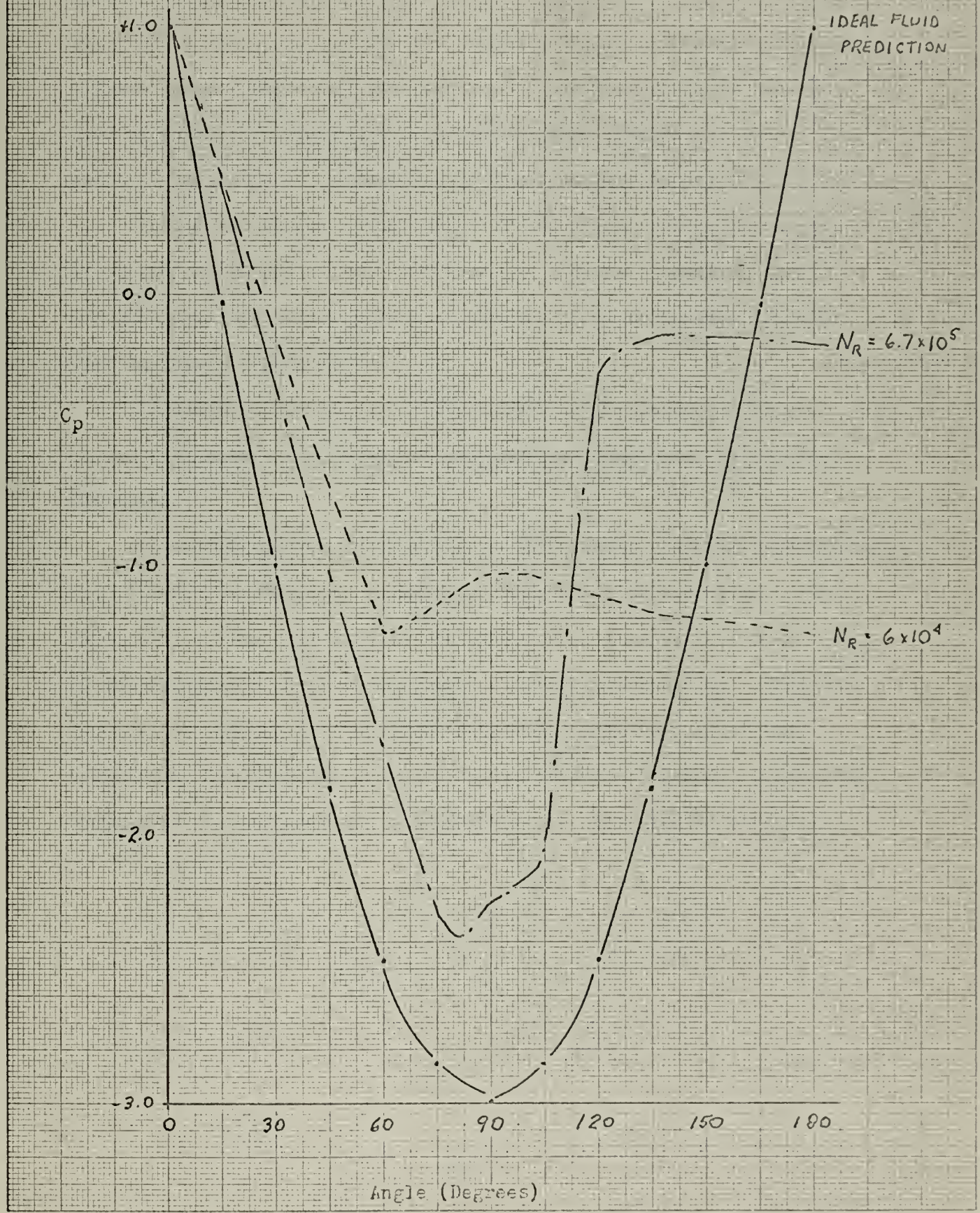

The variation of C_p around the surface of a cylinder is a direct function of the Reynold's Number of the flow. Beginning with the leading stagnation point, the boundary layer thickness increases until at some point along the surface the pressure gradient becomes such that the flow separates from the cylinder producing a wake. The point of separation is controlled by the Reynold's Number of the flow.

As seen in Figure I, the point of separation can be placed in the region of 70-80° of rotation from the leading stagnation point for low Reynold's Number flow to a maximum of approximately 103° for high Reynold's Number flows.

If condensation were to affect the boundary layer thickness around a cylinder, the amount of condensation could also effect the thickness.

An experiment was conducted in a rectangular aluminum test section. The cylinder was inserted through one side via a packing gland. The other side of the test section was fitted with a window for observation. In the cylinder's surface was placed a static pressure tap. This tap was used to measure the pressure around the circumference of the cylinder by rotating the cylinder to the desired position. A detailed drawing of the test section and cylinder are presented in Figure II.

FIGURE II

DETAIL DRAWING OF TEST SECTION AND CYLINDER

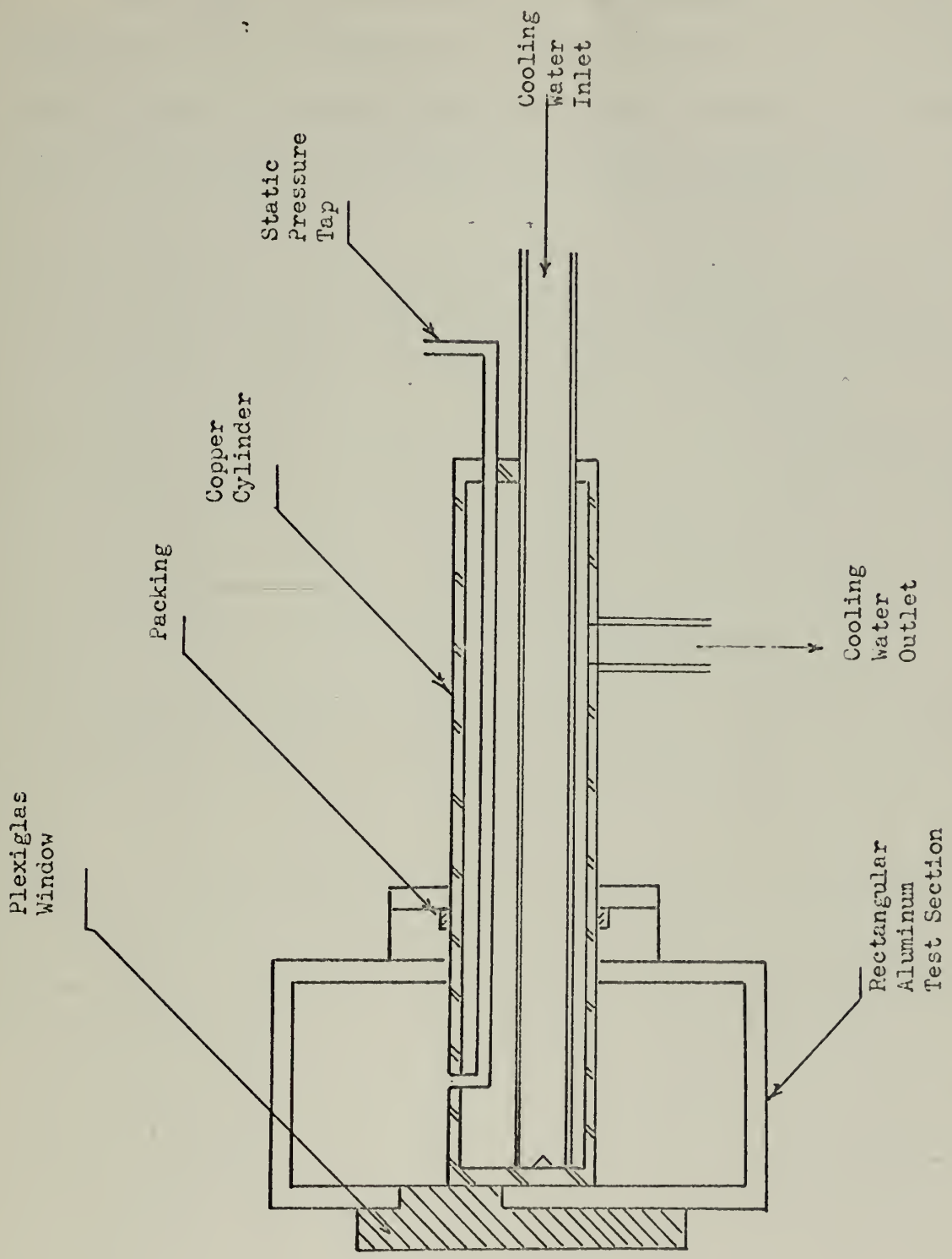

This thesis will be devoted to the measurement of the pressure coefficient around a cylinder in a streaming flow for three condensation rates in order to determine whether or not any variation in the patterns exist and if any do exist, whether or not they are significant.

CHAPTER II

ANALYSIS OF FLOW ABOUT A CYLINDER

1. Cylinder in an Infinite Streaming Flow

Using an irrotational, non-viscous fluid as an ideal model of the flow field, potential flow theory provides an analysis technique to determine the velocity at any point in the field. A stream function consisting of that for a doublet and a streaming flow will represent a cylinder in an infinite medium.

$$\psi = V_o \sin\theta \left[r - R^2/r\right]$$

$$\text{then } V_\theta = -\frac{\partial \psi}{\partial r} = -V_o \left[1 - R^2/r^2\right] \sin\theta$$

$$\text{but if } P_o + 1/2\rho\, V_o^2 = p_\theta + 1/2\rho\, V_\theta^2$$

$$\text{then } C_p = \frac{p_\theta}{1/2\rho\, V_o^2} = 1 - \frac{V_\theta^2}{V^2}$$

$$= 1 - 4 \sin\theta$$

This idealized model of the flow pattern around the cylinder will serve as a maximum to which the measured values of the pressure coefficient can be compared. This pressure coefficient distribution is plotted in Figure I.

2. Cylinder in a Finite Streaming Flow with Walls

Again using potential theory with the aid of two images to create the walls near the central cylinder, a pressure coefficient distribution around the cylinder can be found numerically at a few points around the circumference.

POTENTIAL THEORY IMAGE LOCATIONS

FIGURE III

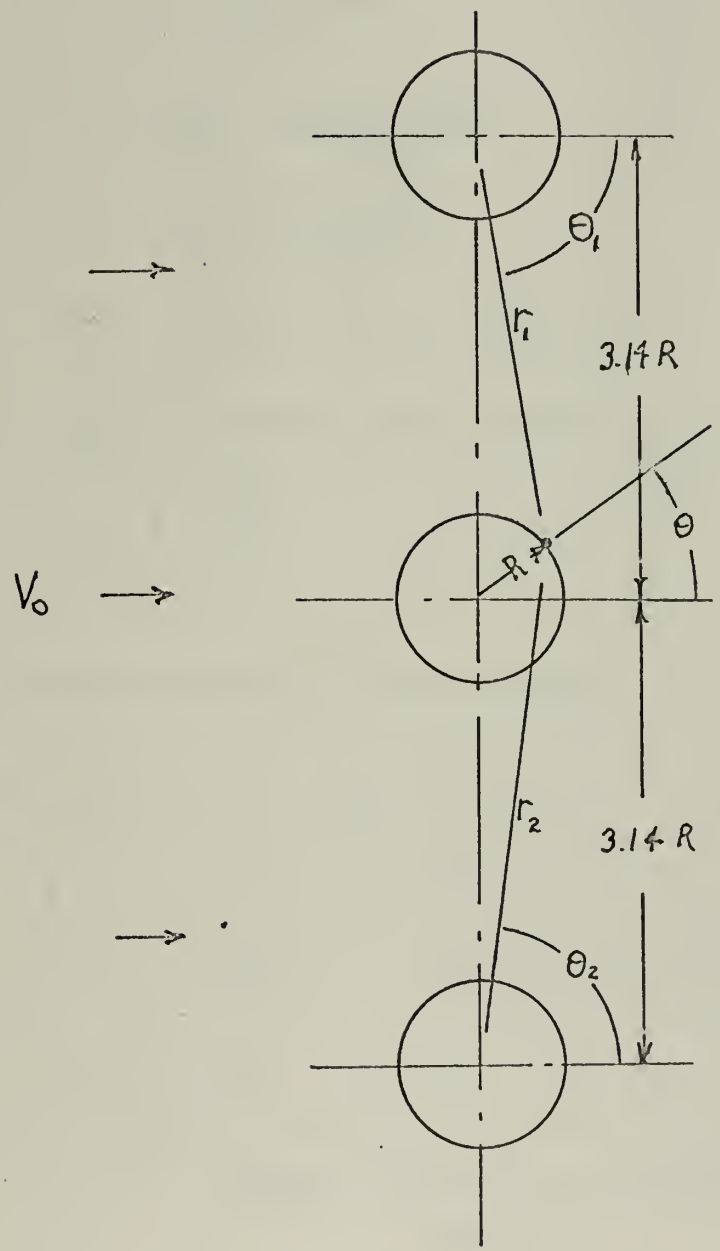

Using linearity and superimposing the three velocity equations

$$V_\theta = - V_o \left[1 + \frac{R^2}{R^2}\right] \sin\theta - V_o \left[1 + \frac{R^2}{r_1^2}\right] \sin\theta_1$$

$$- V_o \left[1 + \frac{R^2}{r_2^2}\right] \sin\theta_2$$

where $$\theta_1 = \tan^{-1} \frac{(3.14 - \sin\theta)}{\cos\theta}$$

$$\theta_2 = \tan \frac{(3.14 + \sin\theta)}{\cos\theta}$$

$$r_1^2 = R^2 \left[\cos^2\theta + (3.14 - \sin\theta)^2\right]$$

$$r_2^2 = R^2 \left[\cos^2\theta + (3.14 + \sin\theta)^2\right]$$

using $$C_p = 1 - \frac{V_\theta^2}{V_o^2}$$

the results are tabulated in Table I below.

Degrees	0	30	60	90	120	150	180
V_θ	0	$-.971\ V_o$	$-1.631\ V_o$	$-1.84\ V_o$	$-1.631\ V_o$	$-.971\ V_o$	0
V_θ^2	0	$+.943\ V_o$	$-2.562\ V_o$	$-3.388\ V_o^2$	$-2.562\ V_o^2$	$+.943\ V_o^2$	0
C_p	1.0	.057	-1.562	-2.388	-1.562	.057	1.0

PRESSURE COEFFICIENT CALCULATION

TABLE I

This is an approximate solution in order to judge the affect of walls on the pressure coefficient distribution. An infinite number of images and the corrections for the flattening of the stagnation stream line from its cylindrical shape were not considered warranted for this approximation because the walls were so distant.

FIGURE IV

SINGLE CYLINDER WITH FAR WALLS PRESSURE RESULTS

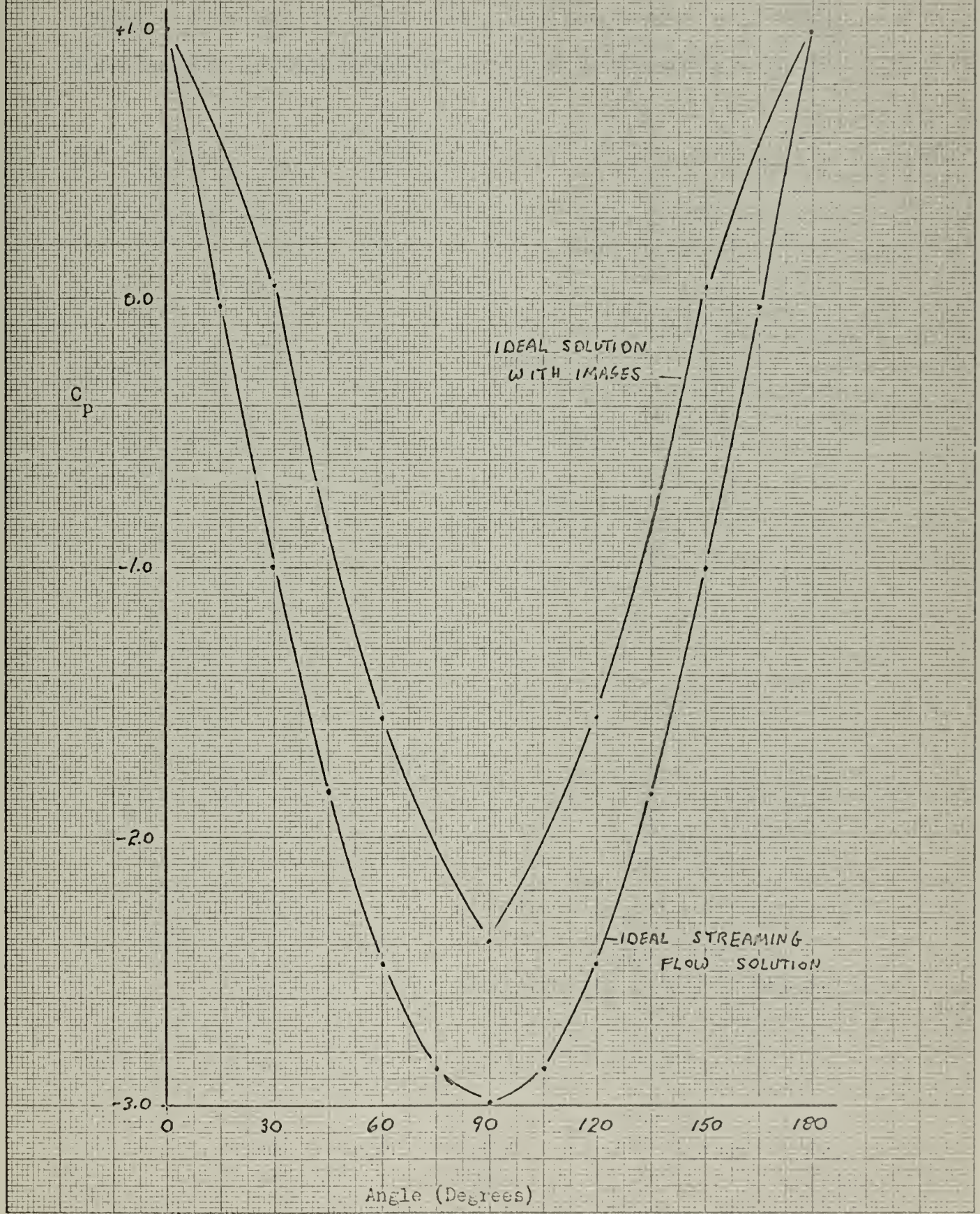

Robertson [5] states that when the image is twice the nominal cylinder radius from the wall, the cylinder is elongated about 1.6%. As can be seen from the analysis, the amount of distortion is small.

CHAPTER III

EXPERIMENTAL PROCEDURE

1. Description of Apparatus

In order to measure the pressure distribution around a cylinder while in a cross flow, the experiment was designed to provide a pressure tap in the cylinder surface midway between the walls of the test section. A 7/8" diameter copper cylinder was provided with a loose packing gland around it in order that the pressure distribution could be achieved by rotating the cylinder to the desired angular position. Condensation on the surface of the cylinder was caused by supplying cooling water to the interior of the cylinder assembly.

A test section was constructed from 1/8" thick aluminum extruded rectangular tubing. The interior dimensions were 1 1/2" by 2 3/4". The overall length of the test section was 48 inches with the cylinder placed about mid-length and in the middle of the channel. A honeycomb flow straightener was placed at the beginning of the test section to provide a uniform flow condition across the test section. A window was provided in the wall at the end of the cylinder to allow visual studies of the condensation patterns around the cylinder.

2. Instrumentation

To measure the Reynold's Number of the flow a standard ASME square edged thin orifice was placed in the flow. This orifice was placed in the center of the rectangular section. Pressure

2. Instrumentation (Cont'd)

taps were placed one diameter upstream and one-half diameter downstream from the orifice. These taps lead to a mercury differential manometer and to an open manometer to determine the state of the steam downstream of the orifice. The steam at this point was assumed to be saturated. As a comparison, the pressure differential measured with the cylinder pressure tap at the stagnation point was reduced to a mass flow rate. As calculated in Appendix II, both were of the same order of magnitude.

The rotating pressure tap of the cylinder was coupled to a static pressure tap in the wall two diameters upstream of the cylinder. This arrangement allowed an averaging of any pressure fluctuations from the unregulated steam supply and made calculations of the pressure coefficient very convenient. The two taps were coupled by a differential manometer filled with Meriam fluid (Specific gravity 2.95).

The remaining portion of the manometer legs were initially filled with water and then individually supplied with water in order to insure an outflow through the tap. This procedure caused inconsistent readings so the fluid was changed from water to air. This technique was intended to preclude any further inconsistencies caused by resistance pressure drops. The outflow was also intended to prevent erratic readings due to any condensation of steam in the manometer legs.

Condensation rates are indicated indirectly by the amount of cooling water provided the cylinder. A Fisher & Porter "Lab Kit"

2. Instrumentation (Cont'd)

rotometer No. FP-3/8-13-G-25 was used to measure the cooling water supplied. The standard conversion table supplied with the "Lab Kit" reduced the readings to flow rates. Condensate velocities are computed in Appendix III.

3. Technique

To begin each data run, the bleed fluid to the manometer lines was adjusted in a "zero steam flow" condition to allow for an outflow in the legs and no reading across the manometers.

First the mercury manometer across the orifice meter was adjusted in this manner. Then the same procedure was followed for the cylinder and wall tap manometer. The amount of fluid outflow was adjusted to the minimum required to maintain an outflow for all the positions of the cylinder tap.

The first attempts in the experiment were made with water as the bleed fluid in the manometer lines. Attempts to regulate the flow through the cylinder and wall taps using water were unsuccessful. The imprecision of the regulating valves caused fluctuations in the manometer readings. Even when the fluctuations were steadied the data runs were not consistant.

Theoretically the pressure drop caused by surface tension of the liquid across the mouth of the pressure tap could be the cause of the inconsistencies. Calculations were made and the magnitude of the pressure drops were of the order of two inches of water. Because this is the same order of magnitude as the desired results, the fluid for the manometer bleed was changed to air. By using air,

3. Technique (Cont'd)

the valve regulation was improved and the surface tension lessened. This change stabilized the fluctuations of the manometers and provided consistent data.

With the use of air as the bleed fluid for the manometer lines, the initial setting of the pressure in each leg was made more easily. One leg was pressurized by dropping approximately one centimeter of Meriam fluid, then the other pressurized to level the manometer fluid. This procedure produced the minimal pressure on each leg consistent with the requirement to maintain an outflow for all positions of the taps in the flow. The stagnation pressure difference measured in centimeters of Meriam fluid of the manometer varied from 2.9 to 3.65.

As indicated in the results section, the magnitude of the reading affected the results of the experiment. Finer regulation of the valves supplying bleed air to the manometer legs could not be accomplished.

After all the adjustments had been made on the bleed air to the manometer legs, the steam flow was adjusted to a given rate by setting the appropriate differential across the mercury manometer. The readings for each data run were measured at 15° increments from 0° (leading stagnation point) to 180°. These points were obtained by rotating the cylinder such that the pressure tap was located at each of these points. An external indicator was used to attain each setting. This was done for each of the three condensation rates. The three condensation rates were as follows: None: 0 cc/min. Light: 53-120 cc/min. Heavy: 830 or over cc/min.

4. Schematic Diagram

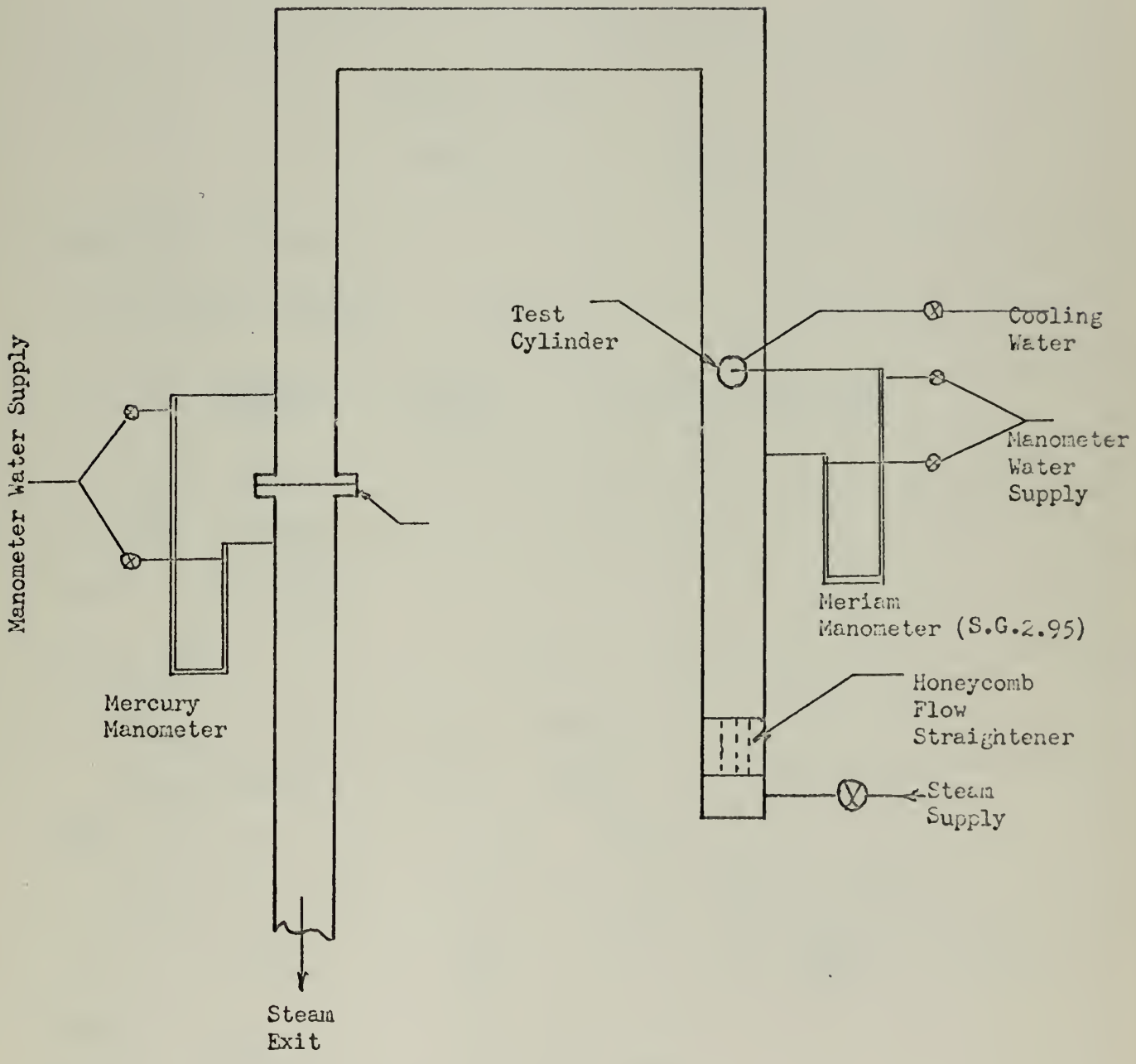

Figure V

5. Sample Calculation

Angle from Stagnation Point (0)	ΔH_{abs} (cm)	ΔH_{hg} (cm)	H_{left} cm	H_{right} cm	$\dot{m}_{water}$	ΔH_{abs} no flow cm
0	10.1	10.8	31.85	28.20	7.0	25.00

SAMPLE RAW DATA

TABLE II

Simplified Calculation

$$\dot{m} = ID^2 \sqrt{h_w/v} \qquad \text{Eq 3.1}$$

if $\beta = \frac{d \text{ orifice}}{D \text{ pipe}} = \frac{1.25}{1.945} = .64$; then I = 98.18 (6)

$D = 1.945$ in

$D^2 = 3.79$ in^2

Then $\dot{m} = 372 \sqrt{h_w/v}$

To calculate v

ΔH_{abs} (no flow) = 25.0 cm Meriam

ΔH_{abs} (measured) = 10.1 cm Meriam

Then $h_m = 25.0 - 10.1 = 14.9$ cm Meriam

$h_w = h_m(S.G.-1) = 5.87(1.95) = 11.4$ in $H_2O = .955$ ft

$P = \gamma_{water} h = 62.4 \frac{lbf}{ft^2} \times .955 \text{ ft} = 59.6 \frac{lbf}{ft^2} = .414$ psig

Therefore $P_{orifice} = 14.7 - .414 = 14.3$ psia

Then v for saturated vapor from Steam Tables(7)

$$v = 27.51 \ \frac{ft^3}{lbm}$$

Therefore using Equation 3.1

$$\dot{m} = 372 \sqrt{h_w/27.51} \quad \text{where } h_w = 12.57 \left\{ \frac{10.8 \text{ cm}}{2.54 \text{ cm/in}} \right\} = 53.25 \text{ in. wate}$$

$$= 372 \sqrt{\frac{53.25}{27.51}} = 518 \ \frac{lbm}{hr.}$$

however $N_R = \rho \frac{VD}{\mu} + \frac{\dot{m}}{A} \frac{D}{\mu}$

$$= 518 \ \frac{lbm}{hr.} \times \frac{1}{.0287 \ ft^2} \times \frac{.0625 \ ft}{1} \times \frac{1}{.0295} \ \frac{lbm}{HR-FT.}$$

$$= 38,200$$

To calculate pressure coefficient

$$C_p = \frac{p}{1/2 \ \rho \ V_o^2} = \frac{\Delta H_i}{\Delta H_{zero}} = \frac{3.65}{3.65} = 1.0$$

To calculate cooling water from Handbook by Fisher Porter

$$\dot{m} = 7.0$$

$$= 155 \text{ cc/min}$$

FIGURE VI

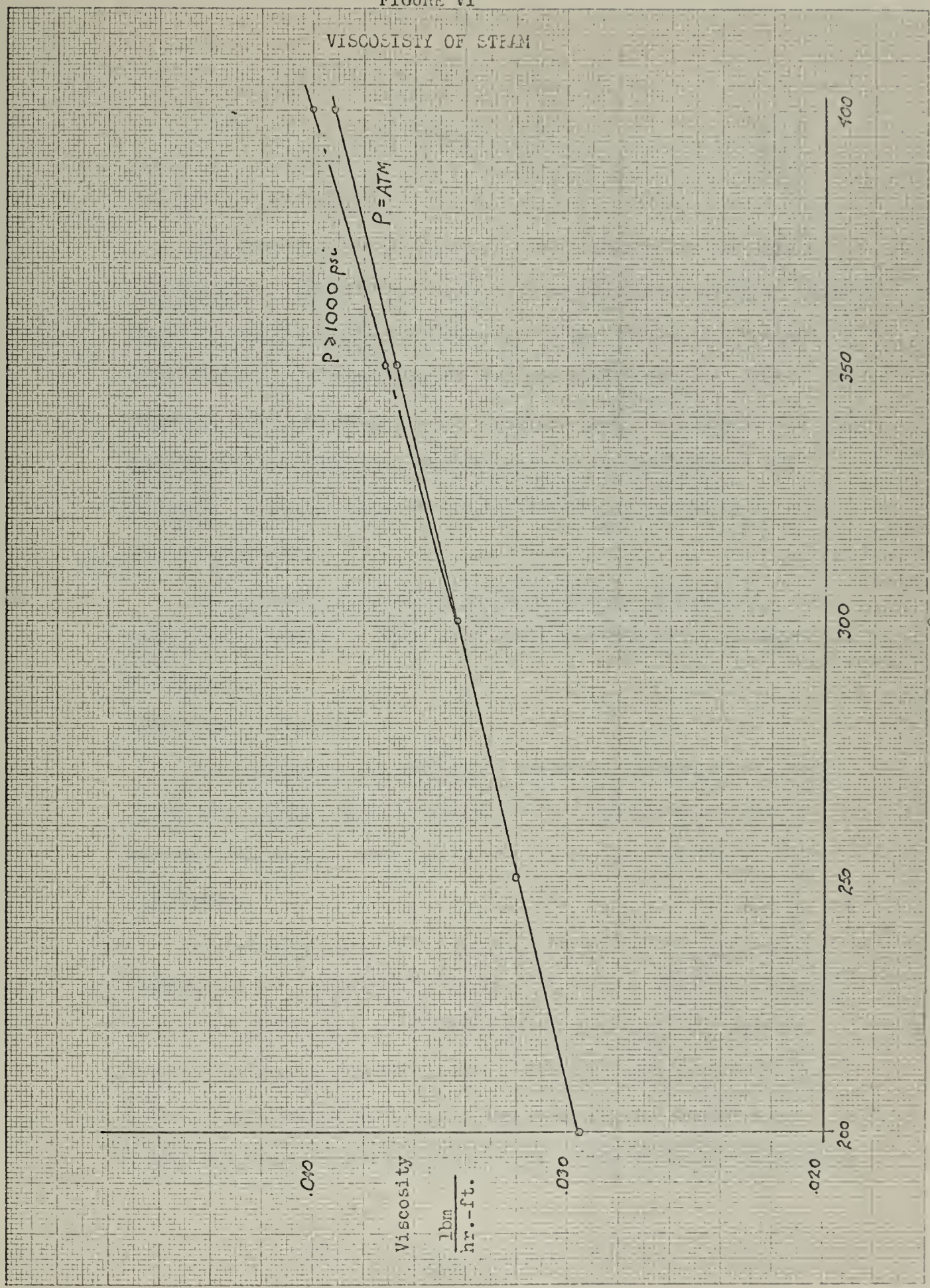
VISCOSITY OF STEAM
P = ATM
P ≥ 1000 psi
Viscosity
lbm / hr.-ft.
.040
.030
.020
200
250
300
350
400
TEMPERATURE (°F)

CHAPTER IV

RESULTS

1. Presentation of Results

The results of this experiment are presented in the form of a series of six graphs representing the individual test runs. Each graph is presented with the following data: the ideal streaming flow solution, the experimental pressure coefficient, and the remaining flow parameters. All test runs were conducted at the same approximate Reynold's Number based on the diameter of the cylinder. A single graph of the three most consistant data runs is also presented.

The wall potential solution is calculated in Appendix I and summarized in Table I. Data from other researchers is reproduced in Figure I.

2. Discussion of Results

The experiment was originally conceived to determine whether or not any changes could be caused in the pressure distribution around a cylinder by condensation and if so, how significant are the changes.

In the Technique section, the difference in the manometer readings at the stagnation point for the various runs was stated. In the graphic results the differences became evident. Because the stagnation reading was used as a divisor in obtaining all the pressure coefficient readings, a slight difference caused the calculated pressure coefficient to vary. This variation is evident

2. Discussion of Results (Cont'd)

when comparing the readings of all the graphs at any one angular position. Of the six graphs only three are suitably consistant to attempt a composite graphic presentation. These three are reproduced in Figure XIII.

Noting that problems of consistant numerical results exist, the trends of the six individual curves may be discussed. Three areas of each graph are worthy of note: the position and magnitude of the maximum negative pressure coefficient, the magnitude of the pressure coefficient just beyond this point on the circumference of the cylinder (i.e. 90°), and the magnitude of the pressure coefficient in the region of the wake (105°-180°).

The position of maximum negative pressure coefficient is about 75° from the leading stagnation point. During all the test runs the rate of condensation caused no dicernable shift from 75°. However, the magnitude of the negative pressure coefficient at this point always did increase for heavy (830 or greater cc/min.) rates of condensation. The results of the light (53-120 cc/min.) rates of condensation were inconsistant and did not appear to produce sufficient evidence for conclusions.

In the area on the circumference about 90° from the leading stagnation point, the magnitude of the pressure coefficient changes significantly. All data indicates that condensation causes the pressure coefficient to increase negatively. The greater the rate of condensation the greater the magnitude of the pressure coefficient. Comparing the six profiles with Figure I, the change in the shape of

2. Discussion of Results (Cont'd)

the pressure coefficient profile at 90° is not unlike the profile changes when the Reynold's Number increases in a non-condensing flow condition.

The two phase boundary layer caused by condensation appears to roughen the cylinder surface and thus produce pressure coefficient profiles like those of a larger Reynold's Number.

The pressure coefficient in the wake region consistantly decreases in magnitude with increasing condensation rate. This shift in profile is always toward the ideal solution.

It is apparant that the Reynold's Number based on the diameter of the cylinder does not provide a complete discription of the flow around the condensing cylinder. Because the profile is similar to those for larger Reynold's Numbers, it must be concluded that the boundary layer in this experiment is turbulent vice laminar which is the condition usually associated with the Reynold's Number of this experiment. This turbulence was stimulated by the honeycomb and test section walls.

The visual studies conducted through the window were inconclusive. The departure of the condensate from the cylinder clearly marked the point of separation on the cylinder. However, quanitative changes in its position for the various amounts of condensation were not apparant.

Considering the ideal streaming flow solution as a no drag condition, the heavy rates of condensation reduced the drag approximately 9%. Numerical integration of the area differences between

2. Discussion of Results (Cont'd)

the ideal solution, the non-condensing solution, and the heavy condensing solution was used to calculate the reduction.

FIGURE VII

PRESSURE COEFFICIENT PROFILE ONE

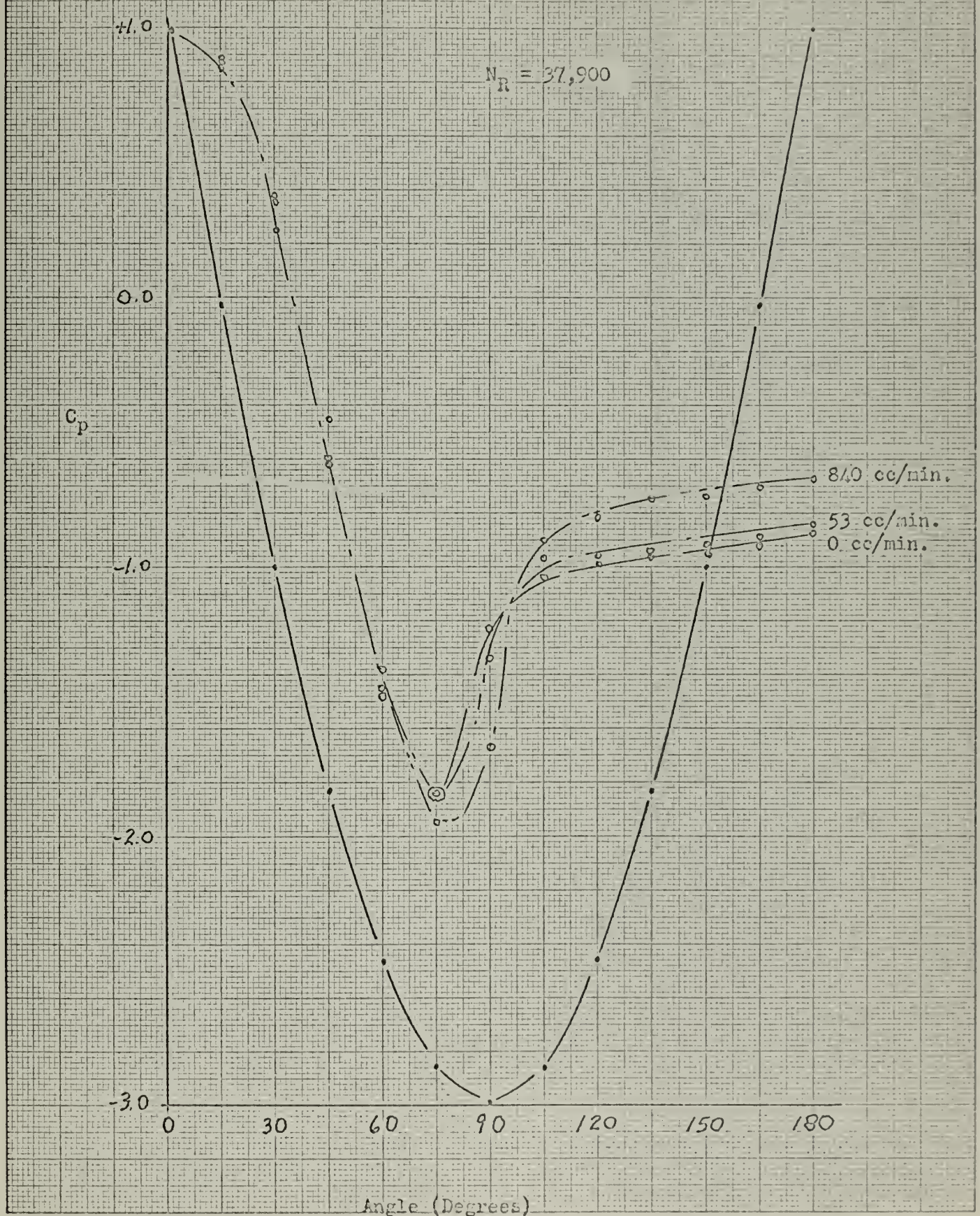

FIGURE VIII

PRESSURE COEFFICIENT PROFILE T-O

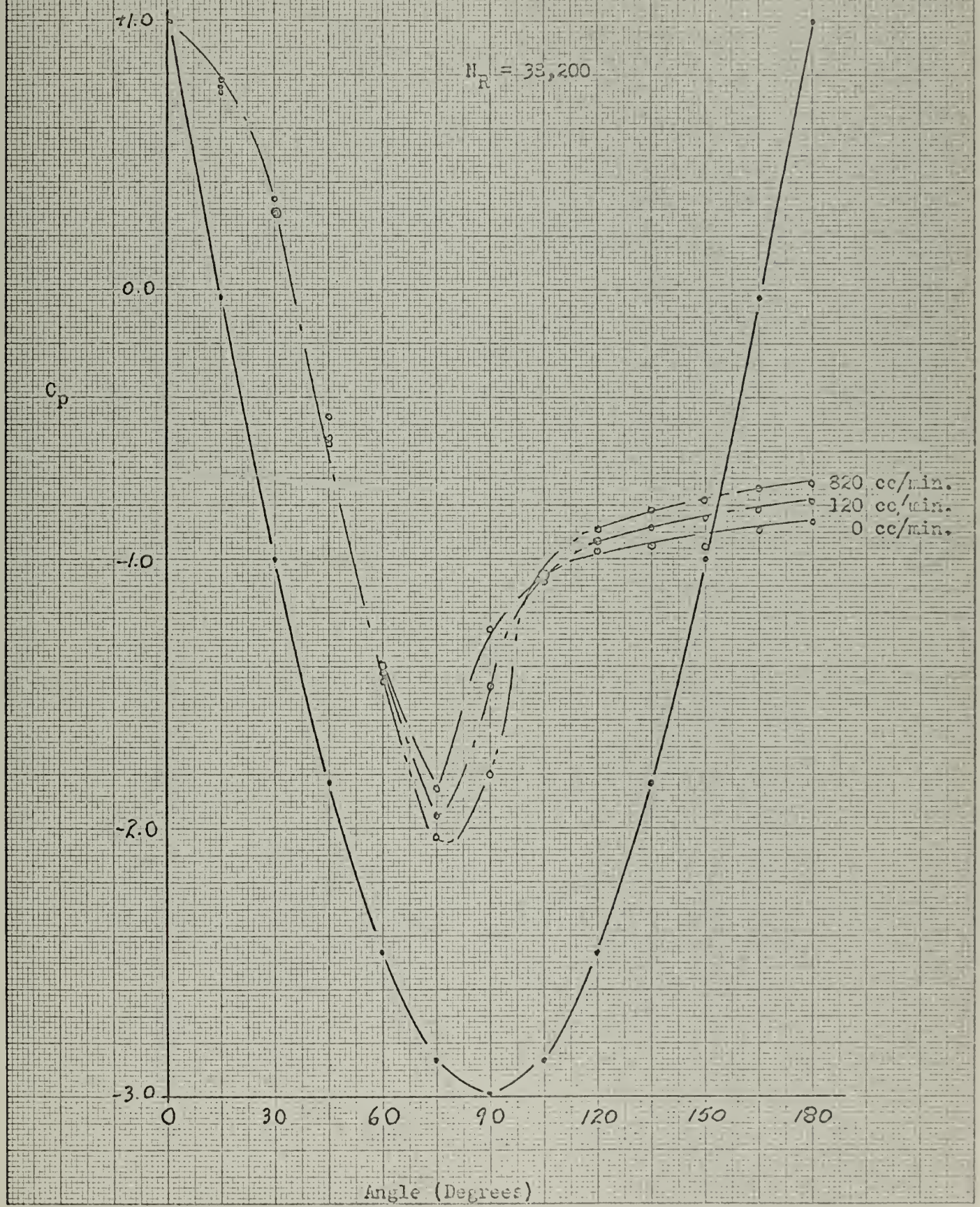

FIGURE 1X

PRESSURE COEFFICIENT PROFILE TABLE

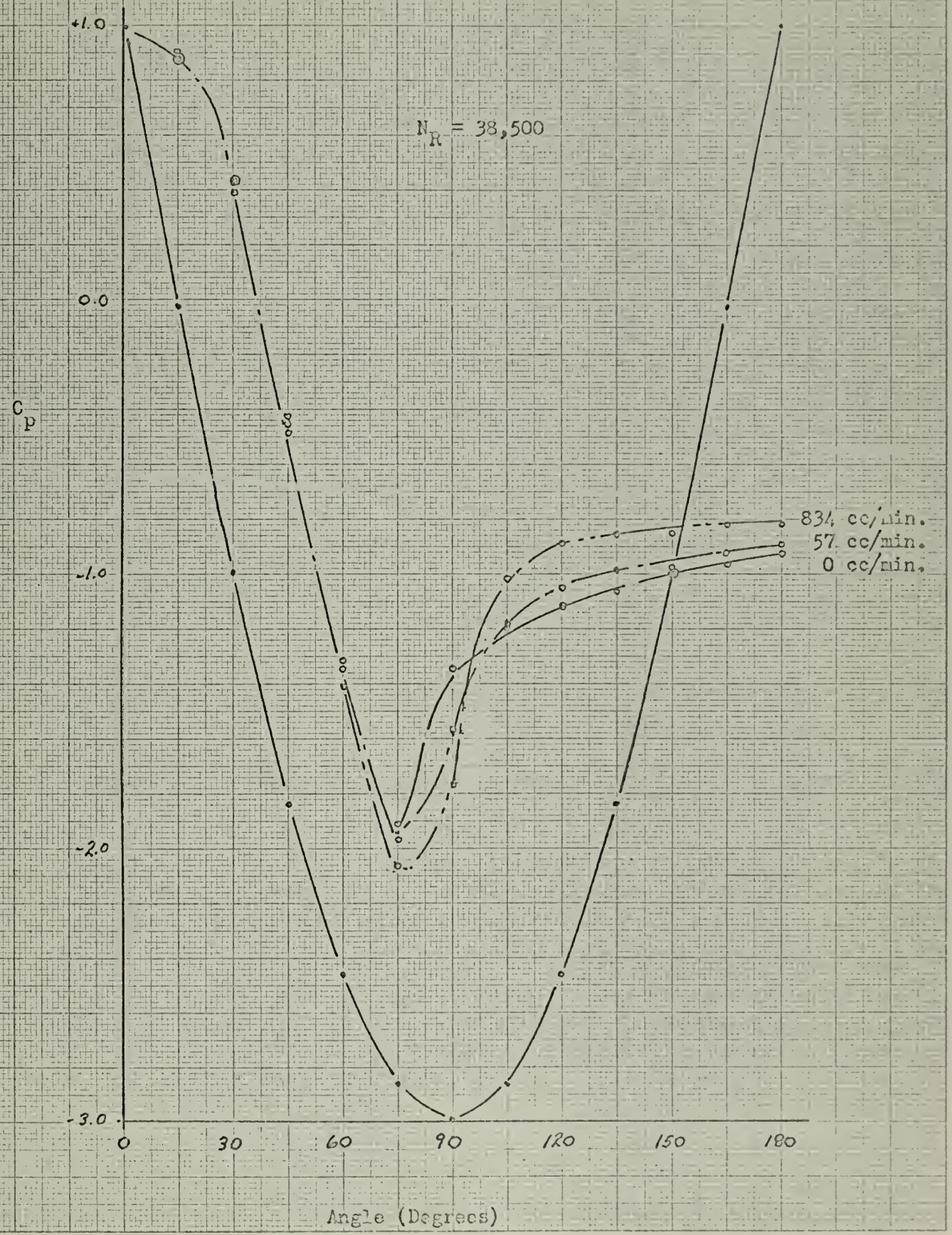

FIGURE X

PRESSURE COEFFICIENT PROFILE FOUR

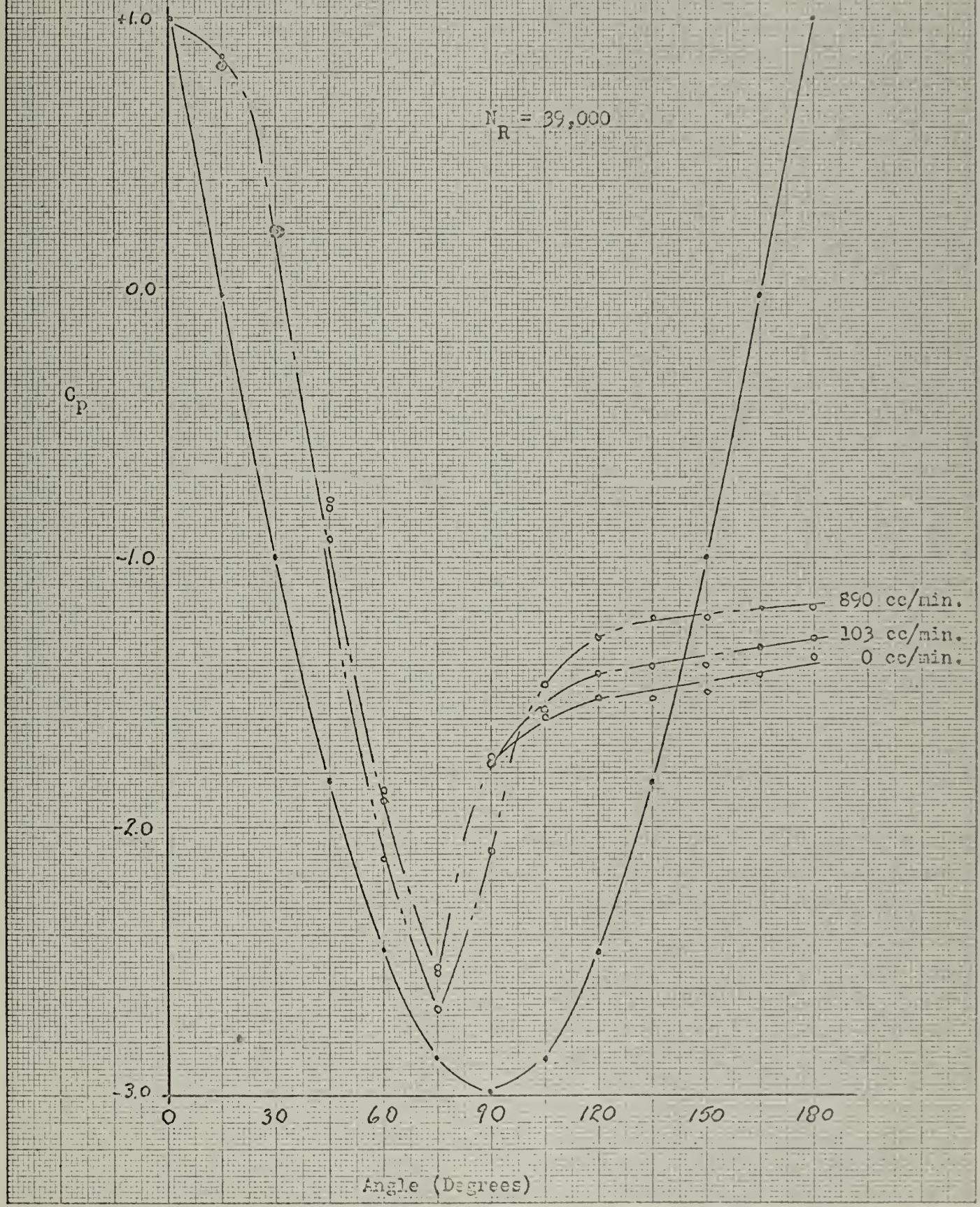

FIGURE XI

PRESSURE COEFFICIENT PROFILE FIVE

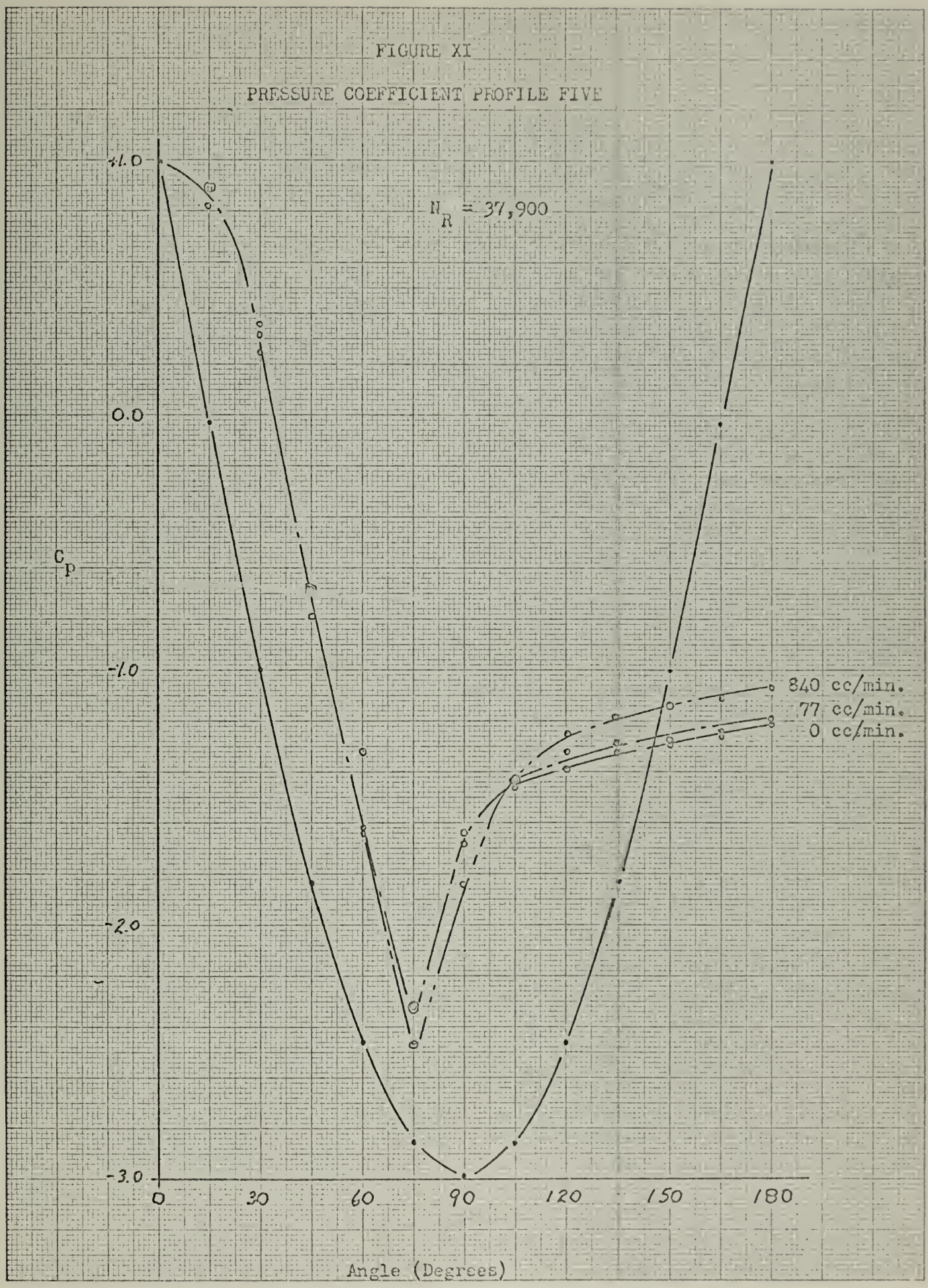

FIGURE XII

PRESSURE COEFFICIENT PROFILE SIX

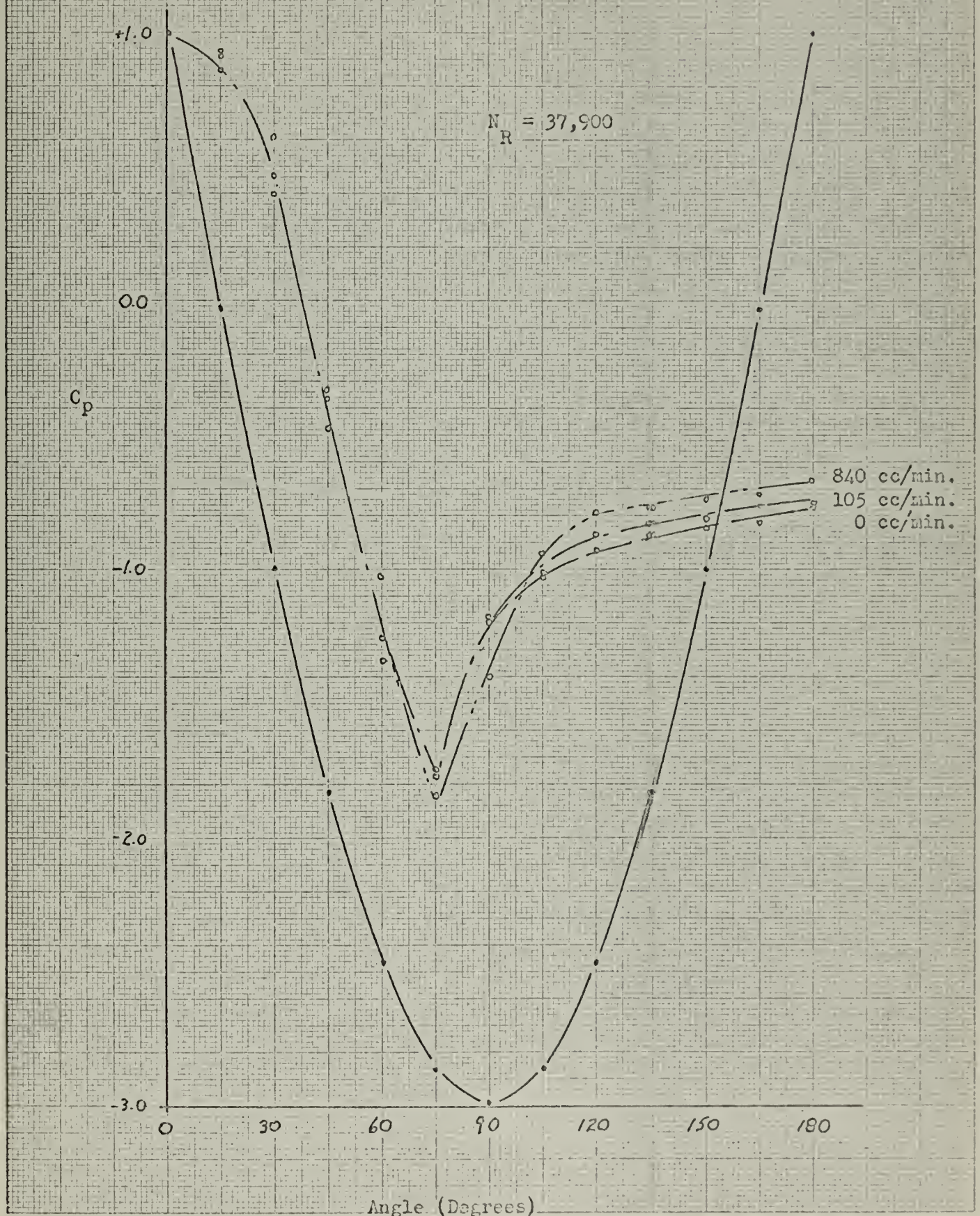

FIGURE XIII

COMBINED PROFILE OF FIGURES
VII, VIII, and IX

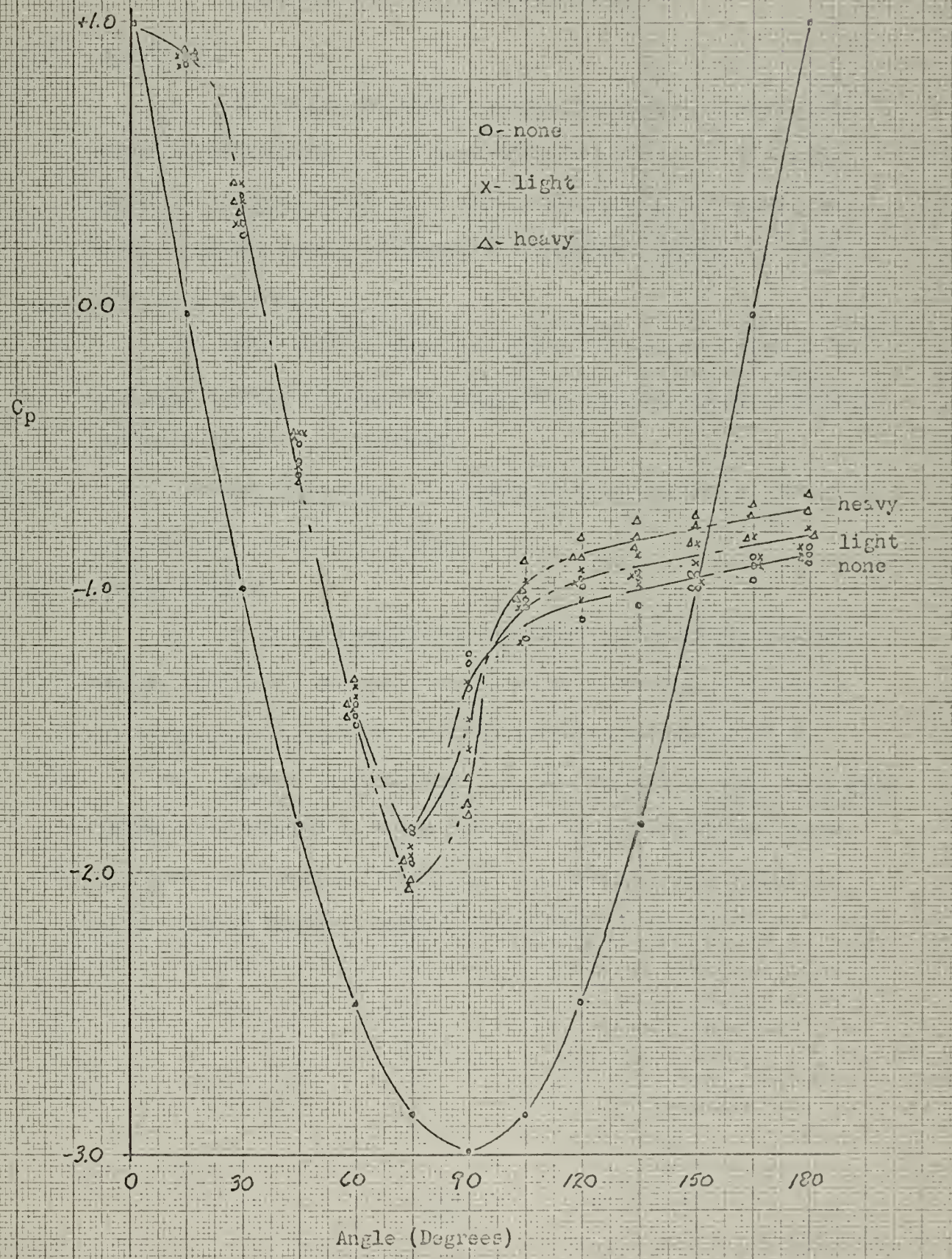

CHAPTER V

CONCLUSIONS AND RECOMMENDATIONS

1. Conclusions

a. With light condensation rates the pressure profile is changed particularly in the area just past the point of maximum negative pressure coefficient and in the area of the wake. In both areas the change of pressure coefficient profile is toward the ideal solution.

b. With heavy condensation rates the pressure profile is not only changed as with the light case, but the maximum negative pressure coefficient increases.

c. With both rates of condensation the amount of change in the pressure profile is modest.

2. Recommendations

a. It is recommended that further investigation into the changes caused by selective condensation surfaces, particularly in cases where a negative pressure gradient exists, be made.

b. Further investigation into the results of this experiment should be attempted on steam devices. In particular the steam diffuser could easily lend itself to a change in its walls to allow them to become a condensing surface.

APPENDIX I

POTENTIAL THEORY SOLUTION WITH IMAGES

$$\psi = V_o r \sin\theta - V_o \frac{R^2}{r} \sin\theta$$

$$v_\theta = -V_o \left[1 + \frac{R^2}{r^2}\right] \sin\theta - V_o \left[1 + \frac{R^2}{r_1^2}\right] \sin\theta$$

$$-V_o \left[1 + \frac{R^2}{r_2^2}\right] \sin\theta_2$$

where $\theta_1 = \tan^{-1} \frac{(3.14 - \sin\theta)}{\cos\theta}$

$$\theta_2 = \tan^{-1} \frac{(3.14 + \sin\theta)}{\cos\theta}$$

$$r_1^2 = R^2 \cos^2\theta + R^2(3.14 - \sin\theta)^2$$

$$r_2^2 = R^2 \cos^2\theta + R^2(3.14 + \sin\theta)^2$$

θ	0°	30°	60°	90°
$\sin\theta$	0.0	.50	.866	1.0
$\cos\theta$	1.0	.866	.50	0.0
$3.14 - \sin\theta$	3.14	2.64	2.274	2.14
$3.14 + \sin\theta$	3.14	3.64	3.806	4.14
$\tan^{-1}\theta_1$	3.14	3.05	4.55	∞
θ_1	72.35°	71.85°	77.6°	90°
$\tan^{-1}\theta_2$	3.14	4.2	7.62	∞
θ_2	72.35°	76.6°	82.5°	90°
$\sin\theta_1$	-.953	-.950	-.977	-1.0
$\sin\theta_2$	+.953	+.973	+.991	+1.0

$\cos^2\theta$	1.0	.75	.25	0
$(3.14 - \sin\theta)^2$	9.54	6.97	5.18	4.58
$(3.14 + \sin\theta)^2$	9.54	13.26	14.48	17.18
$R^2 [\cos^2\theta + (3.14 - \sin\theta)^2] = r_1^2$	10.54 R^2	7.72 R^2	5.43 R^2	4.58 R^2
$R^2 [\cos^2\theta + (3.14 + \sin\theta)^2] = r_2^2$	10.54 R^2	14.01 R^2	14.73 R^2	17.18 R^2
R^2/r_1^2	.0948	.1296	.1845	.2182
R^2/r_2^2	.0948	.0713	.0678	.0582
$1 + R^2/r_1^2$	1.0948	1.1296	1.1845	1.2182
$1 + R^2/r_2^2$	1.0948	1.0713	1.0678	1.0582
$(1 + R^2/r_1^2) \sin\theta_1$	-1.042	-1.072	-1.158	-1.218
$(1 + R^2/r_2^2) \sin\theta_2$	+1.042	+1.043	+1.057	+1.058
$(1 + R^2/R^2) \sin\theta$	+0	+1.0	+1.732	+2.0
V_θ	- 0 V_o	-.971 V_o	-1.631 V_o	-1.840 V_o
V_θ^2	0 V_o^2	+.943 V_o^2	2.562 V_o^2	3.388 V_o^2

then $$C_p = 1 - \frac{V_\theta^2}{V_o^2}$$

C_p	1.0	.057	-1.562	-2.388

APPENDIX II

MASS RATE OF FLOW COMPUTED FROM STAGNATION POINT DATA

1. Calculation of Mass flow rate

$$p_o = p_s + 1/2\ \rho\ V_o^2$$

$$V_o^2 = \frac{2}{\rho \text{steam}}\ (p_o - p_s)g_o = 2v_{st}\ (p_o - p_s)g_o$$

$$= 105{,}500\quad \Delta H(\text{ft})$$

$$= 105{,}500\quad (2.95)\quad \frac{3.65\ \text{cm}}{2.54\ \text{cm/in}}\ \cdot\ \frac{1\ \text{ft}}{12\ \text{in}}$$

$$= 37{,}200\ \text{ft}^2/\text{sec}^2$$

$$V_o = 193\ \text{ft/sec}$$

Therefore $\dot{m} = \rho VA$

$$\dot{m} = \frac{V}{v_{st}}\ A = \frac{193\ \text{ft/sec} \times .0287\ (\text{ft}^2)}{27.1\ \frac{\text{ft}^3}{\text{lbm}}}$$

$$= .204\ \frac{\text{lbm}}{\text{sec}}$$

$$\dot{m} = 740\ \frac{\text{lbm}}{\text{hr}}$$

as calculated from orifice data

$$\dot{m} = 522\ \frac{\text{lbm}}{\text{hr}}$$

2. Discussion

Considering that the exact state of the steam at the cylinder is not known, and that the cylinder is of finite size, the calculation

of the mass flow is not exact. The calculation of mass flow at the orifice is based on a circular cross section of piping. Because the test section is rectangular, the mass flow is not exact.

APPENDIX III

CONDENSATION VELOCITY CALCULATION

This calculation of the velocity of condensation perpendicular to the cylinder surface is approximate and only to obtain the order of magnitude of the velocity.

Using $q = AU\ (\Delta T)$

where $\frac{1}{U} = \frac{1}{h_\ell} + \frac{1}{h_{sc}} + \frac{x_w}{k_w} + \frac{1}{h_{st}}$

$$= \frac{1}{1000} + \frac{1}{1000} + \frac{.0625}{219(12)} + \frac{1}{1000}$$

$$= \frac{3}{1000} + .0000238$$

$$= .003$$

$$U = \frac{1000}{3} = 333$$

then $q = \pi D\ L\ U\ (\Delta T)$

$= 1430$ btu/hr

but $\dot{m} = \frac{q}{h_{fg}} = \frac{1430 \text{ btu/hr}}{970 \text{ btu/lb}} = 1.48 \frac{\text{lb}}{\text{hr}}$

then $V = \frac{\dot{m}}{\rho A} = 1380$ ft/hr $= .38$ ft/sec

This is negligible.

APPENDIX IV

EXPERIMENTAL DATA

1. Pressure Coefficient Profile One

Angle from Stagnation Point	ΔH cm	C_p	$\dot{m}$ H_2O cc/min	ΔH cm	C_p	$\dot{m}$ H_2O cc/min	ΔH cm	C_p	$\dot{m}$ H_2O cc/min
0	3.65	1.0	0	3.65	1.0	140	3.65	1.0	840
15	3.1	.85	0	3.2	.88	110	3.2	.87	840
30	0.9	.25	0	1.4	.38	91	1.35	.37	840
45	-2.2	-.60	0	-1.65	-.45	80	-2.25	-.62	840
60	-5.4	-1.48	0	-5.05	-1.65	62	-5.3	-1.45	840
75	-6.7	-1.84	0	-6.7	-1.84	50	-7.1	-1.95	840
90	-4.5	-1.23	0	-4.9	-1.34	40	-6.1	-1.67	840
105	-3.8	-1.04	0	-3.55	-.97	30	-3.3	-.90	840
120	-3.6	-.99	0	-3.55	-.97	18	-2.95	-.81	840
135	-3.5	-.96	0	-3.45	-.95	15	-2.75	-.75	840
150	-3.45	-.95	0	-3.35	-.92	15	-2.70	-.74	840
165	-3.35	-.92	0	-3.25	-.89	15	-2.55	-.70	840
180	-3.15	-.87	0	-3.1	-.85	15	-2.5	-.69	840
Average	--	--	0	--	--	53	--	--	840

$N_R = 37,900$

2. Pressure Coefficient Profile Two

Angle from Stagnation Point	ΔH cm	C_p	$\dot{m}$ H_2O cc/min	ΔH cm	C_p	$\dot{m}$ H_2O cc/min	ΔH cm	C_p	$\dot{m}$ H_2O cc/min
0	3.6	1.0	0	3.6	1.0	155	3.6	1.0	840
15	3.1	.85	0	3.05	.84	140	3.2	.88	840
30	1.05	.29	0	1.05	.29	120	1.25	.34	830
45	-2.10	-.53	0	-2.05	-.56	120	-1.7	-.47	820
60	-5.3	-1.45	0	-5.2	-1.42	120	-5.1	-1.40	840
75	-6.75	-1.85	0	-7.1	-1.95	120	-7.4	-2.03	815
90	-4.6	-1.26	0	-5.4	-1.47	120	-6.55	-1.80	830
105	-3.85	-1.06	0	-3.95	-1.08	120	-3.85	-1.06	810
120	-3.55	-.97	0	-3.4	-.94	115	-3.25	-.89	810
135	-3.45	-.95	0	-3.2	-.88	115	-3.0	-.82	805
150	-3.45	-.95	0	-3.05	-.84	110	-2.85	-.78	815
165	-3.25	-.89	0	-2.95	-.81	105	-2.70	-.74	815
180	-3.1	-.85	0	-2.90	-.79	105	-2.65	-.73	790
Average	--	--	0	--	--	120	--	--	820

$N_R = 38,200$

3. Pressure Coefficient Profile Three

Angle From Stagnation Point	ΔH cm	C_p	$\dot{m}$ H_2O cc/min	ΔH cm	C_p	$\dot{m}$ H_2O cc/min	ΔH cm	C_p	$\dot{m}$ H_2O cc/min
0	3.25	1.0	0	3.25	1.0	155	3.25	1.0	840
15	2.85	.88	0	2.85	.88	110	2.9	.89	840
30	1.25	.39	0	1.4	.43	90	1.4	.43	840
45	-1.6	-.49	0	-1.45	-.45	90	-1.5	-.46	840
60	-4.6	-1.41	0	-4.4	-1.35	80	-4.3	-1.32	840
75	-6.45	-1.97	0	-6.2	-1.91	50	-6.7	-2.06	840
90	-4.4	-1.35	0	-5.1	-1.57	30	-5.8	-1.77	830
105	-3.85	-1.18	0	-3.9	-1.20	30	-3.3	-1.02	835
120	-3.65	-1.12	0	-3.4	-1.05	30	-2.9	-.89	825
135	-3.45	-1.06	0	-3.2	.99	20	-2.75	-.85	840
150	-3.25	-1.0	0	-3.2	.99	20	-2.75	-.85	830
165	-3.15	-.97	0	-3.0	.92	15	-2.65	-.82	830
180	-3.0	-.92	0	-2.9	.89	15	-2.65	-.82	805
Average	--	--	0	--	--	57	--	--	834

N_R = 38,500

4. Pressure Coefficient Profile Four

Angle From Stagnation Point	ΔH cm	C_p	$\dot{m}$ H_2O cc/min	ΔH cm	C_p	$\dot{m}$ H_2O cc/min	ΔH cm	C_p	$\dot{m}$ H_2O cc/min
0	2.9	1.0	0	2.9	1.0	155	2.9	1.0	840
15	2.5	.86	0	2.4	.83	140	2.4	.83	840
30	0.6	.21	0	0.6	.21	140	0.6	.21	840
45	-2.7	-.93	0	-2.3	-.79	110	-2.35	-.81	840
60	-5.4	-1.86	0	-5.5	-1.9	110	-6.15	-2.12	840
75	-7.4	-2.54	0	-7.3	-2.52	95	-7.75	-2.68	840
90	-5.0	-1.74	0	-5.1	-1.76	95	-6.05	-2.09	840
105	-4.6	-1.59	0	-4.55	-1.57	95	-4.25	-1.47	840
120	-4.4	-1.52	0	-4.15	-1.43	90	-3.75	-1.30	840
135	-4.4	-1.52	0	-4.05	-1.40	80	-3.55	-1.22	840
150	-4.35	-1.50	0	-4.05	-1.40	80	-3.55	-1.22	840
165	-4.15	-1.43	0	-3.85	-1.33	80	-3.45	-1.19	840
180	-3.95	-1.37	0	-3.75	-1.30	70	-3.45	-1.19	840
Average	--	--	0	--	--	103	--	--	840

N_R = 39,000

5. Pressure Coefficient Profile Five

Angle From Stagnation Point	ΔH cm	C_p	$\dot{m}$ H_2O cc/min	ΔH cm	C_p	$\dot{m}$ H_2O cc/min	ΔH cm	C_p	$\dot{m}$ H_2O cc/min
0	2.8	1.0	0	2.8	1.0	110	2.8	1.0	840
15	2.5	.89	0	2.5	.89	90	2.3	.82	840
30	.9	.32	0	1.0	.36	90	0.7	.25	840
45	-1.9	-.68	0	-1.9	-.68	90	-2.2	-.79	840
60	-3.7	-1.32	0	-4.5	-1.61	90	-4.6	-1.64	840
75	-6.5	-2.32	0	-6.5	-2.32	90	-6.9	-2.47	840
90	-4.6	-1.64	0	-4.7	-1.68	80	-5.7	-2.04	840
105	-4.1	-1.46	0	-4.0	-1.43	65	-4.0	-1.43	840
120	-3.9	-1.39	0	-3.7	-1.32	65	-3.5	-1.25	840
135	-3.7	-1.32	0	-3.6	-1.29	65	-3.3	-1.18	840
150	-3.6	-1.29	0	-3.6	-1.29	60	-3.76	-1.14	840
165	-3.5	-1.25	0	-3.5	-1.25	50	-3.1	-1.11	840
180	-3.4	-1.21	0	-3.4	-1.21	55	-3.0	-1.07	840
Average	--	--	0	--	--	77	--	--	840

$N_R = 37,900$

6. Pressure Coefficient Profile Six

Angle From Stagnation Point	ΔH cm	C_p	$\dot{m}$ H_2O cc/min	ΔH cm	C_p	$\dot{m}$ H_2O cc/min	ΔH cm	C_p	$\dot{m}$ H_2O cc/min
0	3.5	1.0	0	3.5	1.0	120	3.5	1.0	840
15	3.0	.86	0	3.2	.91	115	3.25	.93	840
30	1.4	.40	0	2.25	.64	110	1.65	.47	840
45	-1.65	-.47	0	-1.25	-.36	105	-1.15	-.33	840
60	-4.7	-1.34	0	-3.55	-1.02	105	-4.45	-1.27	840
75	-6.2	-1.77	0	-6.05	-1.73	105	-6.4	-1.83	840
90	-4.2	-1.20	0	-4.15	-1.18	105	-4.9	-1.40	840
105	-3.6	-1.03	0	-3.55	-1.02	105	-3.3	-.94	840
120	-3.25	-.93	0	-3.05	-.87	105	-2.75	-.79	840
135	-3.05	-.87	0	-2.95	-.84	100	-2.7	-.77	840
150	-2.95	-.84	0	-2.85	-.82	95	-2.6	-.74	840
165	-2.85	-.82	0	-2.7	-.77	95	-2.4	-.70	840
180	-2.70	-.77	0	-2.7	-.77	95	-2.35	-.67	840
Average	--	--	0	--	--	105	--	--	840

$N_R = 37,900$

REFERENCES

1. Lamb, H., Hydrodynamics, Cambridge University Press, 1932.

2. Milne-Thompson, L. M., Theoretical Hydrodynamics, MacMillan Co., New York, 1960.

3. Schlichting, H., Boundary Layer Theory, McGraw-Hill Book Co., New York, 1955.

4. Rohsenow, W. M. and Choi, H. Y., Heat, Mass, and Momentum Transfer, Prentice-Hall, Inc., Englewood Cliffs, New Jersey, 1961.

5. Robertson, J. M., Hydrodynamics in Theory and Application, Prentice-Hall, Inc., Englewood Cliffs, New Jersey, 1965.

6. Flowmeter Computation Handbook, The American Society of Mechanical Engineers, New York, 1961.

7. Keenan, J. H. and Kaye, F. G., Thermodynamic Properties of Steam, John Wiley & Sons, Inc., New York, 1936.